DSC analysis of liquid volume fraction and compressive behavior of the semi-solid Si$_3$N$_4$w/Al–Si composite

S.J. Qu,[a,*] A.H. Feng,[b] L. Geng,[c] Z.Y. Ma[b] and J.C. Han[a]

[a]Center for Composite Materials, Harbin Institute of Technology, Harbin, China
[b]Institute of Metal Research, Chinese Academy of Sciences, 72 Wenhua Road, Shenyang 110016, China
[c]School of Materials Science and Engineering, Harbin Institute of Technology, Harbin, China

The compressive deformation behavior of the semi-solid 20 vol.% Si$_3$N$_4$w/Al–Si composite and corresponding Al–Si alloy has been investigated. The volume fraction of liquid in the semi-solid composite can be measured by DSC analysis. The relationship between the isothermal holding time in the semi-solid state and compressive behavior was investigated in detail. The results indicated that the addition of Si$_3$N$_4$ whisker accelerated the melting of the composite. Strain softening appears during compressive deformation of the semi-solid composite.
© 2007 Acta Materialia Inc. Published by Elsevier Ltd. All rights reserved.

The rheological and mechanical behavior of semi-solid alloys, i.e. superplastic deformation [1], compressive deformation [2,3] and shear deformation [4], has been extensively investigated. It has been pointed out that the liquid phase plays an important role in the high-strain-rate superplasticity (HSRS) [1]. Semi-solid compressive deformation has been carried out for a number of alloy systems, particularly the hypoeutectic Al–Si alloys.

Semi-solid processing offers significant advantages over casting, forging and powder metallurgy techniques, such as reduction of macrosegregations and reduction of porosity [5,6]. Four major semi-solid deformation mechanisms have been proposed: liquid flow, flow of liquid incorporating solid particles, sliding between solid particles and plastic deformation of solid particles mechanisms [7]. From the viewpoint of rheological flow, the semi-solid state alloys behave as viscoplastic, nonlinear solids for the high solid phase volume fraction, but as non-Newtonian fluids for the low solid phase volume fraction [3]. The viscosity of the semi-solid metals depends on the volume fraction and morphology of the solid phase and the shear strain rate [4]. During

semi-solid state deformation, the liquid cannot carry any load and the load is transferred to the existing solid dendrite network [8]. Therefore, the volume fraction of liquid significantly affects the rheological behavior of alloys during semi-solid deformation.

Generally, three available methods, i.e. a conventional quenching and image analysis method, calculations using simplistic solidification models of the Lever rule and the Scheil model, and a proposed differential thermal analysis method coupled with mathematical modeling, have been used frequently to determine the volume fraction of the solid phase [9,10]. However, the quenching and image analysis method has several experimental difficulties, especially for composites. Furthermore, the applicability of model calculation is often restricted by the lack of physical parameters of the semi-solid alloys [9].

Differential scanning calorimetry (DSC), which involves the measurement of heat flow corresponding to the nucleation and growth processes [11], has been widely applied to the study of precipitation in aluminum alloys [12,13]. Melting and solidification of the metal are first-order phase transitions, including phase transition temperature and latent heat of fusion, which can be measured by DSC technique. In the present paper, DSC analysis was used for the systematic characterization of the liquid volume fraction. Partial remelting

experiments were carried out to determine the influence of temperature and holding time on the semi-solid compressive properties.

The 20 vol.% Si_3N_4w/4032Al composite was fabricated by squeeze casting. The composition of the 4032Al alloy was 11.5Si–1.0Mg–0.5Cu–0.5Ni (wt.%). The volume fraction of liquid was measured by non-isothermal DSC using the STA449C DSC equipment. Semi-solid compressive deformation behavior was studied on a Gleeble1500 Thermal Simulator. The compressive specimens were 6 mm in diameter and 9 mm in length. All the specimens were compressed to a thickness of 2 mm, with a reduction in thickness of 77.8%. After isothermal holding for various times, ranging from 1 to 40 min, at 540–560 °C, the specimen was deformed at a constant strain rate of $0.37\,s^{-1}$.

DSC results indicated that there were two melting endotherm peaks, of the composite and 4032Al alloy, respectively (Fig. 1). Based on the Al–Si phase diagram, the basic microstructure was primary aluminum solution and eutectic Al–Si phase for 4032Al alloy. The first endothermic peak, at the lower temperature, corresponded to the melting of the eutectic Al–Si phase and the second endothermic peak, at the higher temperature, referred to the melting of the primary aluminum solution (Fig. 1a). It was observed that the second peak of the composite features a narrow peak resulting in the lower enthalpy (Fig. 1b). Obviously, the melting of the composite was completed earlier than that of the 4032Al alloy. Therefore, the addition of Si_3N_4 whisker accelerated the melting of the composite. The possible reasons were more interfaces and the morphology change of primary aluminum solution from dendrite-like to equiaxed due to the addition of Si_3N_4 whisker [14]. It has been well documented that the presence of the particles in particle–reinforced composites accelerates the globularization of the solid phase during semi-solid deformation [15].

As proposed by some investigators from their non-isothermal DSC analyses, the fraction of transformation heat released is proportional to the degree of transformation f at any given time t (or temperature T) [11]:

$$f(T) = \frac{\int_{T_S}^{T} \frac{\partial h}{\partial t}\mathrm{d}t}{\int_{T_S}^{T_E} \frac{\partial h}{\partial t}\mathrm{d}t} = \frac{\int_{T_S}^{T} \Delta H \mathrm{d}t}{\int_{T_S}^{T_E} \Delta H \mathrm{d}t}, \tag{1}$$

where t_S and t_E are the transformation start and end times, respectively, T_S and T_E are the transformation temperatures corresponding to t_S and t_E, respectively, and ΔH is the measured transformation heat released at any given time t (or temperature T).
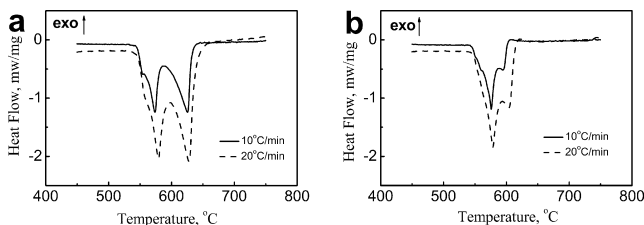
Table 1. Transition enthalpy of the Si_3N_4w/4032Al composite and the 4032Al alloy

Transition enthalpy (J g^{-1})	Heating rate (°C min^{-1})	
	10	20
4032Al alloy	66.07	129.7
Si_3N_4w/4032Al composite	32.20	71.10

Taking into account the expression in Eq. (1), the transformation degree of the liquid in the composite and the 4032Al alloy can be calculated from the respective DSC experimental curves and plotted as a function of temperature $f(T)$.

The enthalpy of the phase transitions (Table 1) was evaluated using a numerical method and computational programming. The results indicated that the transition enthalpy of both the composite and the 4032Al alloy increased with increasing heating rate. Also, the addition of the Si_3N_4 whiskers significantly decreased the enthalpy of the primary aluminum, while it had no obvious influence on the enthalpy of the eutectic Al–Si phase compared with the 4032Al alloy.

Figure 2 shows the plots calculated by Eq. (1) and the subsequent numerical method and computational programming using the DSC experimental data, illustrating the relationship between the volume fraction of liquid and temperature (Table 2). During heating, when the temperature exceeded the initial melting temperature, melting started at the grain boundaries due to the melting of eutectic Al–Si phase, and then the primary aluminum began to melt with prolonged holding time. It was found that enthalpy of the composite was lower than that of the 4032Al alloy. Therefore, compared with the 4032Al alloy, the volume fraction of liquid for the composite increased much faster with increasing temperature.

The DSC curves of the isothermal holding at 540 °C for 1 h indicated that there was no obvious endothermic peak of the composite and the 4032Al alloy, illustrating no melting of the eutectic Al–Si phase (Fig. 3).
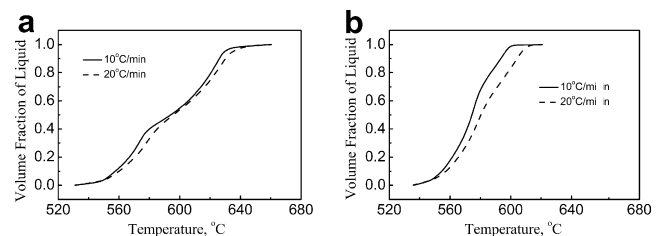
Figure 2. Relationship between the volume fraction of liquid and temperature for (a) the 4032Al alloy and (b) the Si_3N_4w/4032Al composite.

Figure 1. DSC analysis results of the 4032Al alloy (a) and the Si_3N_4w/4032Al composite (b).

Table 2. The volume fraction of liquid for the Si_3N_4w/4032Al composite and the 4032Al alloy

Volume fraction of liquid (%)	540 °C	560 °C	580 °C	600 °C
4032Al	1.2	13.3	40.2	55.5
Si_3N_4w/4032Al	1.6	18.3	67.9	96.2
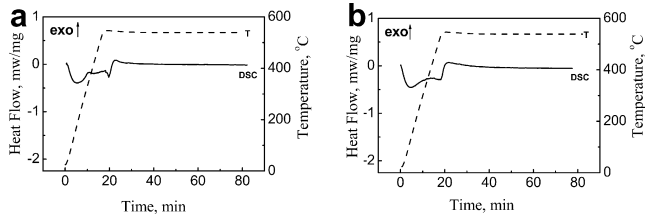
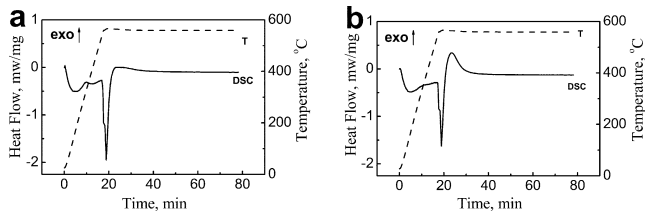**Figure 3.** DSC curves of isothermal holding at 540 °C for 1 h for (a) the 4032Al alloy and (b) the Si₃N₄w/4032Al composite.

Figure 4. DSC curves of isothermal holding at 560 °C for 1 h for (a) the 4032Al alloy and (b) the Si₃N₄w/4032Al composite.

In contrast, an obvious melting endothermic peak has been observed in the isothermal holding curves at 560 °C for 1 h of the composite and the 4032Al alloy (Fig. 4). The isothermal DSC condition was responsible for only one melting endothermic peak. The results indicated that ∼30 min of isothermal holding is necessary for the volume fraction of liquid to reach its equilibrium state (Fig. 4). The volume fraction of liquid will not increase even after a prolonged isothermal holding time. It is worth noting that an additional exothermic peak, corresponding to the reaction between the Si₃N₄ whisker and the aluminum matrix, was present when the holding time was ∼25 min (Fig. 4b).

The semi-solid state alloys are characterized by the coexistence of solid and liquid phases at thermal equilibrium [16]. With a low volume fraction of liquid, liquid wets the grain boundaries by a thin film that solidifies epitaxially [5]. The volume fraction of liquid was close to 13.3% for the 4032Al alloy and 18.3% for the composite at 560 °C (Table 2). When the 4032 aluminum alloy was compressed at 560 °C for various isothermal holding times, partial melting was found to start at the grain boundaries. Meanwhile, the primary aluminum dendrite arms coarsened during hot compression [14]. With increasing isothermal holding time, liquid uniformly surrounded the solid grain; at 20 vol.% liquid, the average thickness of the liquid film around a spherical grain 50 μm in size was only 1.8 μm [5].

As shown in Figure 5, the microstructure exhibited various characteristics from the center to the free surface of the compressed specimens. During semi-solid compressive deformation, only the solid region around the contact die deformed, and the liquid region and solid grains flowed to the free surface in the middle part of the material, with the outermost material being separated from the surface [17]. With an isothermal holding time of 20 min, the equiaxed grain size at the center area of the compressive specimen was ∼35 μm, with occasional unmelted silicon particles scattered within the matrix (Fig. 5a). However, in the side area the number
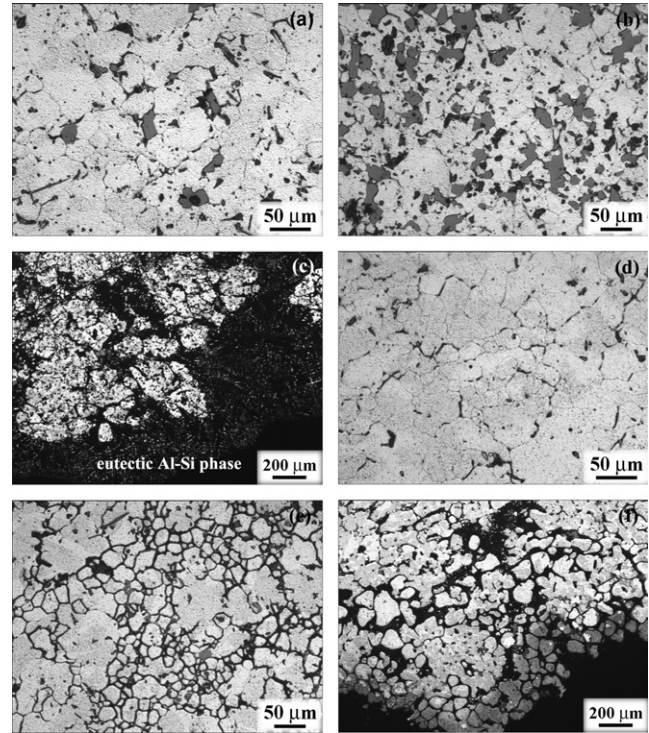

Figure 5. Microstructure of the compressed 4032Al alloy isothermal holding at 560 °C for 20 min (a–c) and 30 min (d–f).

of unmelted silicon particles increased. Compared with the center area, the grain size was slightly smaller in the side area due to the effective pinning of the silicon particles (Fig. 5b). Furthermore, the surface of the specimen was broken away during compression by the liquid flow towards the surface, resulting in the liquid segregation around the edge area (Fig. 5c). When the isothermal holding time was increased to 30 min, there was no obvious unmelted silicon particles in either the center or the edge area of the compressed sample (Fig. 5d–f). With increasing isothermal holding time, macro-separation was hence successfully reduced due to the homogeneous distribution of the liquid phase (Fig. 5e and (f)). Accordingly, the optimal isothermal holding time was deemed to be ∼30 min for the 4032Al alloy.

The flow stress of the 4032Al alloy increased slightly with increasing holding time (Fig. 6a). However, the true stress–true strain curve of the composite is typically characterized by a peak flow stress followed by a stable flow stress (Fig. 6b). Strain softening appears during compressive deformation of the composite in the semi-solid state.
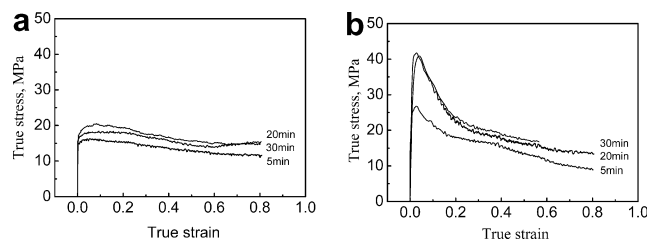

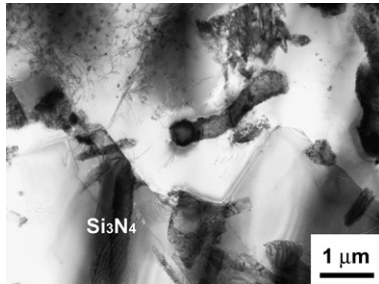**Figure 6.** True stress–true strain curves compressed at 560 °C for different times of (a) the 4032Al alloy and (b) the Si₃N₄w/4032Al composite.

Figure 7. TEM image of dynamic recrystallization in the Si_3N_4w/ 4032Al composite compressed at 560 °C for 30 min.

During compressive deformation of the composite, the whiskers must move and rotate to accommodate the deformation of the matrix. When the composite was compressed at 560 °C, the liquid phase appears preferentially at the reinforcement/matrix interface or the grain boundaries, where it can serve as a lubricant for whisker redistribution. For short isothermal holding, which corresponded to small volume fractions of liquid, the liquid segregation resulted in a significant decrease in the peak flow stress. Meanwhile, the matrix offered less resistance to whisker redistribution. With a prolonged isothermal holding time, there was more time for the liquid to distribute uniformly at the grain boundaries, which contributed to the load transferring from the whisker to the matrix, resulting in the improvement of the flow stress.

Therefore, the redistribution and breakage of the whisker are responsible for the obvious strain softening of the composite [18]. In addition, the dynamic recovery and recrystallization processes occurring within the matrix were also attributed to the strain softening. Figure 7 shows the dynamically recrystallization in the composite compressed at 560 °C for 30 min.

In summary, the following conclusions were reached: (i) the volume fraction of liquid in semi-solid matrix alloys can be measured by DSC analysis; (ii) the addition of Si_3N_4 whisker accelerated the melting of the composite; and (iii) strain softening appears during compressive deformation of the semi-solid composite.

[1] K. Higashi, T.G. Nieh, M. Mabuchi, J. Wadsworth, Scripta Metall. Mater. 32 (7) (1995) 1079.
[2] Y. Chino, M. Kobata, H. Iwasaki, M. Mabuchi, Acta Mater. 51 (2003) 3309.
[3] E.R.D. Freitas, M. Ferrante, Acta Mater. 49 (2001) 3839.
[4] H. Iwasaki, T. Mori, M. Mabuchi, K. Higashi, Acta Mater. 45 (18) (1998) 6351.
[5] E. Tzimas, A. Zavaliangos, Mater. Sci. Eng., A 289 (2000) 228.
[6] W.R. Loue, M. Suery, Mater. Sci. Eng., A 203 (1995) 1.
[7] C.P. Chen, C.Y.A. Tsao, Acta Mater. 45 (5) (1997) 1955.
[8] W.M.V. Haaften, W.H. Kool, L. Katgerman, Mater. Sci. Eng., A 336 (2002) 1.
[9] S.W. Chen, C.C. Huang, Acta Mater. 44 (5) (1996) 1955.
[10] H.K. Jung, C.G. Kang, J. Mater. Process. Technol. 104 (2000) 244.
[11] K.G. Keong, W. Sha, S. Malinov, J. Non-Cryst. Solids 324 (2003) 230.
[12] M.J. Starink, P.J. Gregson, Scripta Metall. Mater. 33 (6) (1995) 893.
[13] H.B. Dong, J.D. Hunt, Mater. Sci. Eng., A 413–414 (2005) 470.
[14] A.H. Feng, L. Geng, J. Zhang, C.K. Yao, Mater. Chem. Phys. 82 (2003) 618.
[15] L.N. Thanh, M. Suery, Mater. Sci. Eng., A 196 (1995) 33.
[16] H.L. Yang, Z.L. Zhang, I. Ohnaka, J. Mater. Process. Technol. 151 (2004) 155.
[17] C.G. Kang, J.S. Choi, K.H. Kim, J. Mater. Process. Technol. 88 (1999) 159.
[18] L. Geng, S. Ochiai, J.Q. Hu, C.K. Yao, Mater. Sci. Engi., A 246 (1998) 302.